ACS APPLIED MATERIALS & INTERFACES

Research Article

www.acsami.org

Facilitated Ion Diffusion in Multiscale Porous Particles: Application in Battery Separators

Young Bum Kim,[†,#] Thanh Tran-Phu,[†,#] Min Kim,[†] Dae-Woong Jung,[†] Gi-Ra Yi,*[,†] and Jong Hyeok Park*[,‡,§]

[†]School of Chemical Engineering and [‡]SKKU Advanced Institute of Nanotechnology, Sungkyunkwan University, Suwon 440-746, Republic of Korea

[§]Department of Chemical and Biomolecular Engineering, Yonsei University, 50 Yonsei-ro, Seodaemun-gu, Seoul 120-749, Republic of Korea

Supporting Information

ABSTRACT: Polyethylene (PE) separators have been the most popular option for commercial Li-ion batteries because of their uniform pore size, high tensile strength, low cost, and electrochemical stability. Unfortunately, PE separators generally suffer from significant dimensional changes at high temperatures, which frequently results in serious safety problems. In this regard, the integration of inorganic nanoparticles with PE separators has been considered to be a promising approach. Here, inorganic nanoparticles with a hierarchical pore structure were coated on a conventional polymer separator. The resultant composite separator exhibited superior Li ion transportation compared with separators coated with mesopore-only nanoparticles or conventional nonporous nanoparticles. The mesopores and macropores act synergistically to improve the electrolyte uptake and ionic conductivity of the inorganic nanoparticles, while other positive aspects such as their thermal and mechanical properties are still maintained.

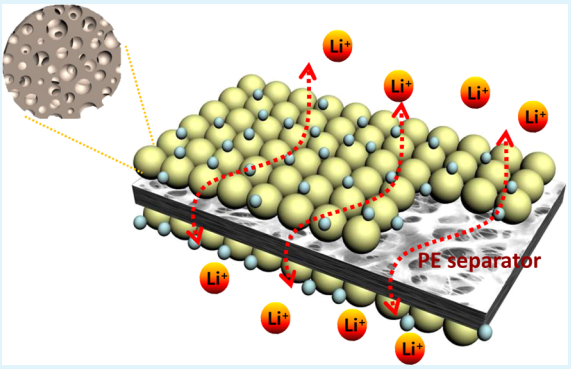

KEYWORDS: *Li-ion battery, membrane, separator, inorganic, safety*

INTRODUCTION

The development of energy storage cells with high-energy capacities will be crucial for powering mobile electronics and electric vehicles (EVs) in the future.[1,2] Because of their reasonable energy densities and cycle stability, Li-ion batteries (LIBs) have rapidly spread into mobile electronics and electric or hybrid-electric vehicle (HEV) applications.[3−8] To expand the application of LIBs, the performance of each battery component has been optimized, including the cathode, anode, electrolyte, and separator. However, less attention has been paid to the development of the separator because separators have been considered passive components that are not directly linked with battery performance. Among the separators that have been developed thus far, polyethylene (PE) separators have been the most popular for commercial LIBs because of their uniform pore size, high tensile strength, low cost, and electrochemical stability.[9−13] Even though commercial PE separators with suitable ion conductivity have been used to maximize the available capacity of the active materials in the two different electrodes, serious concerns exist regarding these separators. These concerns include their intrinsically poor compatibility with conventional polar solvents in liquid electrolytes and their insufficient electrolyte uptake, which result from their hydrophobic surface character and low surface energies. The separator is also relevant to LIB safety because it acts as a physical spacer between the cathode and anode to prevent their direct contact.[14,15] However, the insufficient thermal and dimensional stabilities of PE separators have raised serious concerns over their ability to maintain safe LIBs under abnormal heating or hard internal short conditions. Moreover, the poor mechanical and thermal stabilities of PE separators cause even more severe problems in their application to EVs and HEVs because the high-energy density of large LIB packs is a safety concern.

Recently, many studies have overcome the aforementioned obstacles of PE separators. To improve their poor wetting capabilities and low thermal stabilities, PE separators have undergone many modifications, most of which involve the addition of extra surface layers. Several approaches have been taken, such as coating inorganic nanoparticles (SiO_2 or Al_2O_3) with a poly(vinylidene fluoride-*co*-hexafluoropylene) PVdF−HFP polymer[16−18] or coating a thermally stable thin film on the PE surface.[19−21] Among these approaches, the addition of an inorganic nanoparticle coat with a polymeric binder via a

Received: October 3, 2014
Accepted: January 16, 2015
Published: January 16, 2015

DOI: 10.1021/am506797d
ACS Appl. Mater. Interfaces 2015, 7, 4511−4517

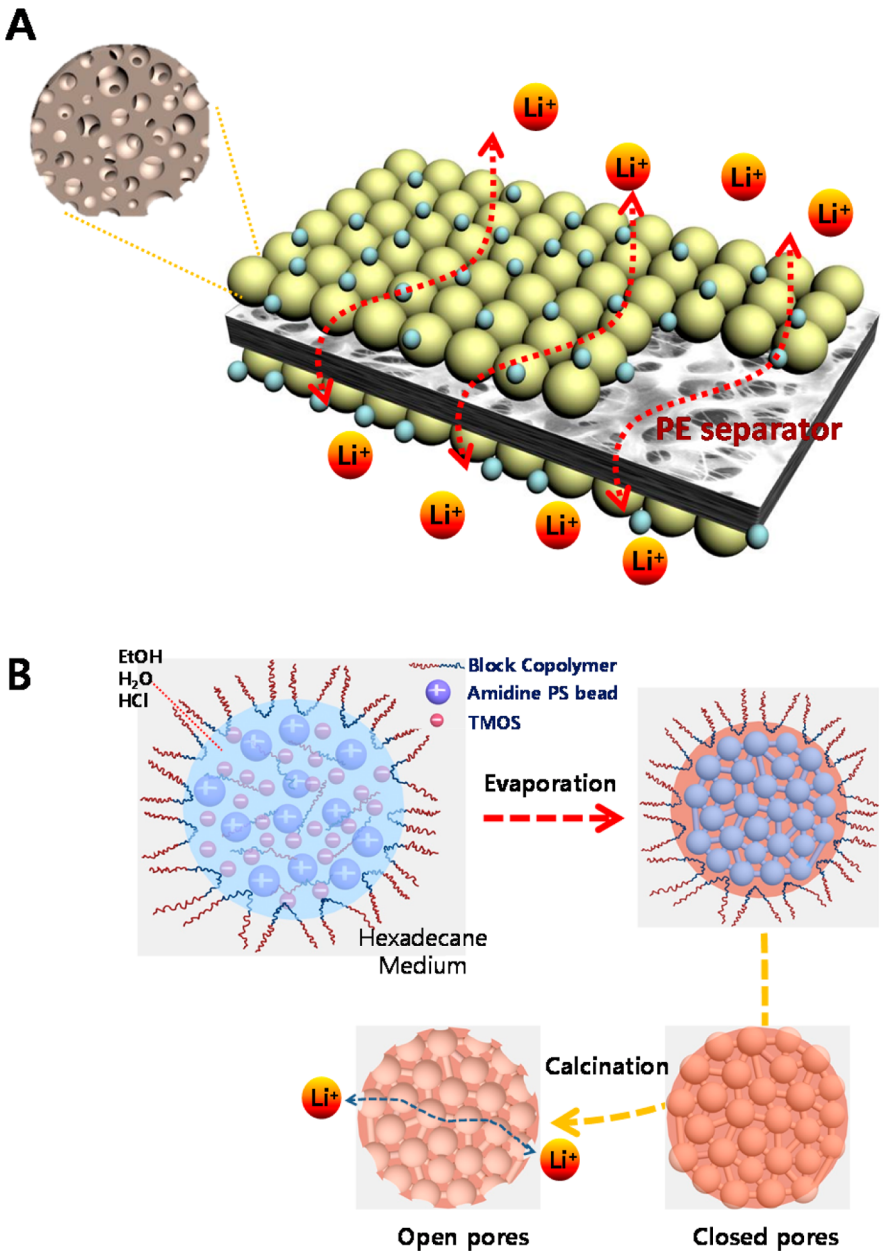

Figure 1. Schematic diagram of (A) the proposed separator coated with multiscale nanoporous particles and (B) procedures for the synthesis of multiscale nanoporous particles.

solution process is a particularly effective way to improve the thermal stability and wettability of pristine PE.[16−18] In general, ionic conductivity is considered to be a key factor of separators. However, the ionic conductance [$G = (\sigma A)/l$, where σ is the ionic conductivity, A is the area, and l is the thickness] of a separator is more crucial than its ionic conductivity, which is normalized to the thickness of the separator. For instance, micropores generated from the interparticle distance of coated inorganic nanoparticles can provide reasonable ionic conductivities, which in turn increase the ionic conductivities of the composite separators (the ionic conductivity of the inorganic nanoparticle layer might be higher than that of PE). However, the inorganic nanoparticle layers on the PE separator tend to offer additional resistance for ionic transportation (resulting in low ionic conductance), thereby giving rise to increased cell resistance. This resistance can diminish the positive effects of the inorganic nanoparticle coating.

In this study, novel inorganic nanoparticles with multiscale pore structures synthesized by a facile approach were coated on PE separators using a simple solution dip-coating method. This technique provided a highly porous nature to the membrane for its application as a separator in LIBs (Figure 1A). Inorganic nanoparticles with both macropores and mesopores yielded superior LIB performance when coated on a PE substrate compared with mesopore-only nanoparticles or conventional nonporous nanoparticles. The combination of mesopores and macropores in the inorganic nanoparticles resulted in synergistic effects that improved the electrolyte uptake and ionic conductivity, while also maintaining other positive effects such as good thermal and mechanical properties. The PE separator coated with inorganic nanoparticles with multiscale pores presented much better LIB performance than neat PE separators.

DOI: 10.1021/am506797d
ACS Appl. Mater. Interfaces 2015, 7, 4511−4517

EXPERIMENTAL SECTION

Preparation of Meso-macroporous, Mesoporous, and Nonporous Silica Particles. Meso-macroporous silica particles were successfully synthesized using a modified version of the emulsion-assisted dual templating process.[22] Typically, 0.2 g of suspension consisting of 10 wt % 250 nm polystyrene (PS) beads (synthesized by additive-free emulsion polymerization[23]) and 10 wt % $HO(CH_2CH_2O)_{20}(CH_2CH(CH_3)O)_{70}(CH_2CH_2O)_{20}H$ (P123) (Aldrich) dispersed in deionized water was mixed with 0.8 g of suspension consisting of 10 wt % 250 nm PS beads dispersed in ethanol. Next, 0.1 mL of 0.01 N HCl (Samchun) was added for 10 min by vigorous stirring at 600 rpm. Then 0.1 g of tetramethylorthosilicate (TMOS, Aldrich) was added for 30 min to obtain the dispersed (water) phase. The continuous (oil) phase was prepared by dissolving 3 wt % AbilEM90 into hexadecane. To obtain water droplets, the water phase was dispersed in the oil phase (volume ratio 1:10) at 22 000 rpm for 15 s using a T10 basic homogenizer (ULTRA-TURAX, IKA, Korea). The resultant emulsion droplets were heated at 90 °C in a 20 mL vial for 2 h using a hot plate stirrer (SMHS-6, Witeg). During the heat treatment process, the water and ethanol inside droplets (water phase) diffused slowly through the oil phase (hexadecane) and then evaporated. Meanwhile, composite particles were formed inside water droplets by sol−gel reaction of the silica precursor (TMOS), self-assembed PS beads, and surfactant (P123).[22] These particles, which contained SiO_2, PS beads, and P123, were collected by centrifugation and washed twice each with isopropanol and ethanol. To eliminate free PS beads and P123, composite particles were calcined at 540 °C for 5 h with a heating rate of 1 °C min^{-1}. The resultant white powder was obtained and characterized. To generate mesoporous silica particles without PS beads (i.e., lacking macropores), 0.1 g of P123 was dissolved into a solution of 0.8 g of methanol and 0.2 g of deionized water. The remainder of the process (from HCl addition until calcination) was performed as described above. Nonporous silica particles were generated by the same procedure, except that P123 was omitted.

Preparation of the PE Separators with Silica Nanoparticles. The silica coating solution was prepared by mixing SiO_2 particles with different morphologies and PVdF−HFP (HFP content = 6 mol %, Arkema) in acetone. The ratio of silica/PVdF−HFP was fixed at 90/10 (wt %/wt %). After PVdF−HFP was first dissolved in acetone, a fixed amount of silica powder was added and the solution was vigorously mixed via ball milling and hand shaking for 2 h. A PE polymer matrix (E16MMS, 18 μm thickness, Donen, Japan) was then coated with the silica nanoparticles via a dip-coating process. The separators were dried at room temperature (35% humidity) to evaporate the acetone and further vacuum-dried at 50 °C for 4 h. Consequently, both sides of the PE separators were coated with a ∼2.7 μm thick layer. Separator thickness was measured using a portable thickness gauge (Mitutoyo, Japan).

Cell Fabrication and Characterization. To measure the electrochemical performance of the separators, an electrolyte solution was prepared containing 1 M $LiPF_6$ and a solvent mixture of ethylene carbonate (EC), dimethyl carbonate (DMC), and ethyl methyl carbonate (EMC) (EC/DMC/EMC = 1/1/1 wt/wt/wt, PuriEL, Soulbrain Co., Ltd., Korea). The composite separator was sandwiched between a 94 wt % mesocarbon microbead anode and a 90 wt % $LiCoO_2$ cathode (4 wt % PVdF binder and 6 wt % Super-P). For the charge−discharge test, the lithium coin cell was assembled as a 2032 battery type. A scanning electron microscope (SEM; JSM-7000, JEOL, Japan), operated at 20 kV, was used to examine separator morphologies. A transmission electron microscope (TEM; JEOL 2000FX), operated at 200 kV, was used to examine the internal structures of the silica nanoparticles. Samples were prepared by adding a silica nanoparticle suspension dropwise onto a TEM grid, after which the grid was dried at 70 °C for 20 min. Nitrogen adsorption desorption isotherms of the silica nanoparticles were measured using a micromeritics system (ASAP 2040). Specific surface areas were determined using a multipoint Brunauer−Emmett−Teller (BET) model[24] in a relative pressure range from 0 to 950 mmHg. The Barrett−Joyner−Halenda (BJH) model[25] was used to calculate the mesopore size distributions and pore volumes and to generate desorption curves. The ionic conductivity (σ) of the separator was determined using an alternating current (ac) impedance spectroscope (CHI-660, CH Instruments, USA) over a frequency range of 0.01−100 kHz. An ac perturbation of 5 mV was applied to the cell. The electrolyte uptakes (%) of the separators were obtained by measuring the masses of the separators before and after soaking in liquid electrolyte solution for 1 h. Electrolyte uptakes were calculated using the following equation: Electrolyte uptake (%) = $(M_f - M_i)/M_i \times 100\%$, where M_i and M_f are the masses of the separator before and after electrolyte soaking, respectively. For the charge−discharge test, the discharge C-rate capability of the cells was examined using a 16-channel automatic battery cycler (WBCS 3000, Wonatech). Batteries were tested by charging to 4.3 V at a 0.2C rate and discharged to 3.0 V at various C-rates ranging from 0.2 to 3.0C.

RESULTS AND DISCUSSION

Spherically shaped, meso-macroporous, and mesoporous silica particles were synthesized in bulk by dual templating inside emulsion droplets. Amidine-encapsulated PS beads and amphiphilic triblock copolymers were simultaneously assembled inside an emulsion with TMOS as a silica source, which forms composite particles during droplet evaporation. Spherical meso-macroporous silica particles were obtained in powder form by thermal sintering to remove free PS beads and triblock copolymers. Macropore size was controlled via the size of the PS beads, although slight pore shrinkage did occur during thermal sintering. During the bulk synthesis, emulsion droplets served as microreactors. The volumes of the droplets were controlled during the reaction by simple evaporation, as shown in Figure 1B. Positively charged PS beads were interconnected with negatively charged silica precursors inside emulsion droplets, leading to a loosely interconnected, gel-like composite. Hence, all reactants remained inside the emulsion during the evaporation process. Mesoporous silica particles were also synthesized in templates without PS beads.

As shown in parts (A) and (B) of Figure 2, meso-macroporous silica particles were successfully synthesized using 250 nm amidine PS beads and a triblock copolymer (P123) as templates for macropores and mesopores, respectively. The pores inside the particles were well interconnected, with partially open windows. The size distribution of the particles was obtained by measuring the diameters of more than 100 particles and is plotted in Figure S1 of the Supporting Information. The average diameter was approximately 600−800 nm. As an alternative, mesoporous silica particles lacking macropores were also synthesized. SEM

DOI: 10.1021/am506797d
ACS Appl. Mater. Interfaces 2015, 7, 4511−4517

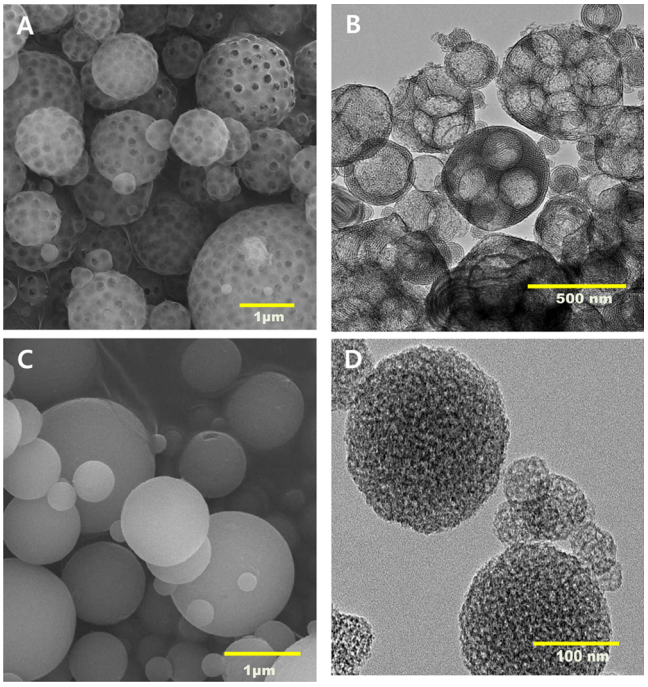

Figure 2. SEM and TEM images of meso-macroporous silica particles (A, B) and mesoporous silica particles (C, D).

and TEM images of these particles are shown in parts (C) and (D), respectively, of Figure 2. The average mesoporous silica particle size was approximately 500–600 nm, as shown in Figure S1. The meso-macroporous silica particles were larger due to the introduction of macropores inside the particles by using 250 nm PS beads.

Nitrogen adsorption–desorption curves for the meso-macroporous and mesoporous silica particles are shown in Figure S2. The BET surface areas of the particles were 541 m^2/g (meso-macroporous silica) and 546 m^2/g (mesoporous silica). It is noteworthy that the BET surface area of the meso-macroporous particles was slightly less than that of the mesoporous particles, presumably due to the macroscale voids in the meso-macroporous particles. A BJH adsorption–desorption experiment was performed to obtain the average mesopore diameter. Since the macropore size was beyond the limit of detection, only mesopores and their size distributions were observed (Figure S3); the average size of these mesopores was 3.6 nm. The silica nanoparticle coating solution for the PE separators was prepared by dispersing the synthesized particles with the PVdF–HFP binder in acetone solvent. To investigate the influence of inorganic particle morphology on LIB performance, three kinds of separators were prepared: meso-macroporous silica nanoparticles on PE, mesoporous silica nanoparticles on PE, and conventional nonporous silica nanoparticles. As a reference PE substrate, a commercial PE separator with a thickness of approximately 18 μm was used (Figure S4). Particle solutions were coated on the PE substrate by a dip-coating method, followed by drying at 25 °C and 40% relative humidity. When the nanoparticles were coated on the PE separator with the aid of a small amount of PVdF–HFP adhesive material, the inorganic particles were uniformly dispersed on top of the PE surface, as shown in Figure 3. Because the inorganic nanoparticle content in the coated layer on the PE separator was 90 wt %, most of the pores in the coating layer could be generated via the interparticle distance in

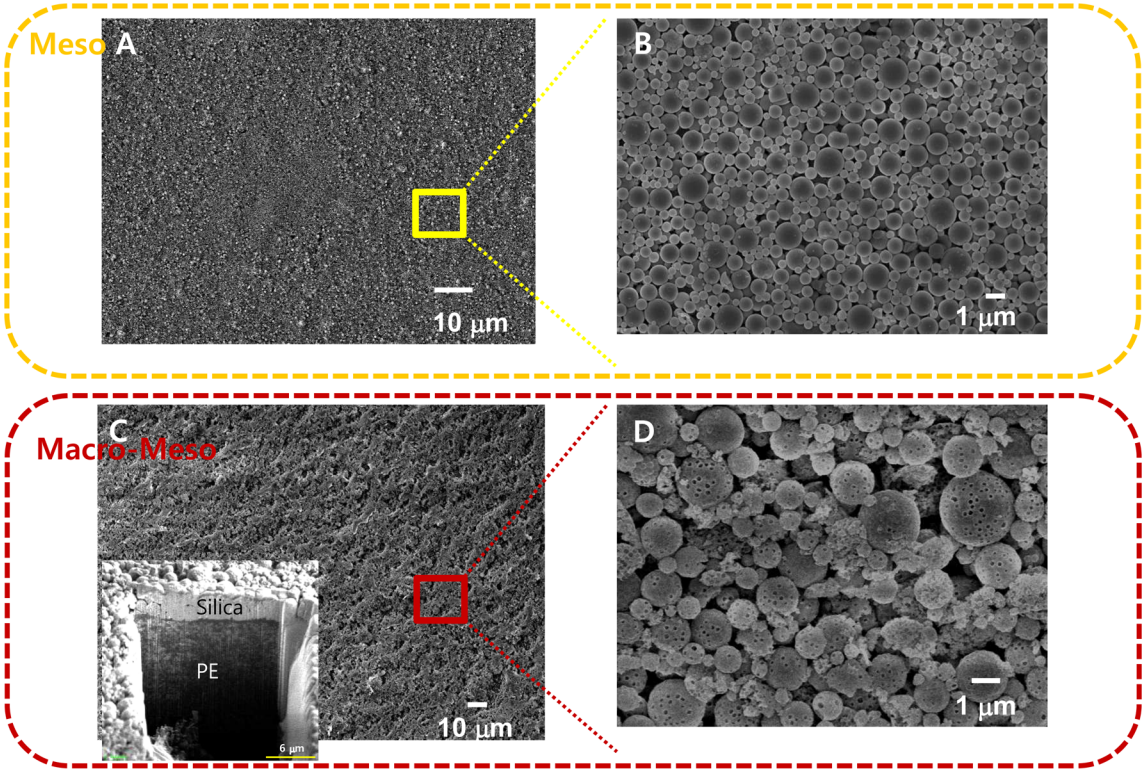

Figure 3. Surface SEM images of mesoporous silica-coated PE (A, B) and meso-macroporous silica-coated PE (C, D) separators. A cross-sectional SEM image using a focused ion beam (FIB) is also shown (C, inset).

DOI: 10.1021/am506797d
ACS Appl. Mater. Interfaces 2015, 7, 4511–4517

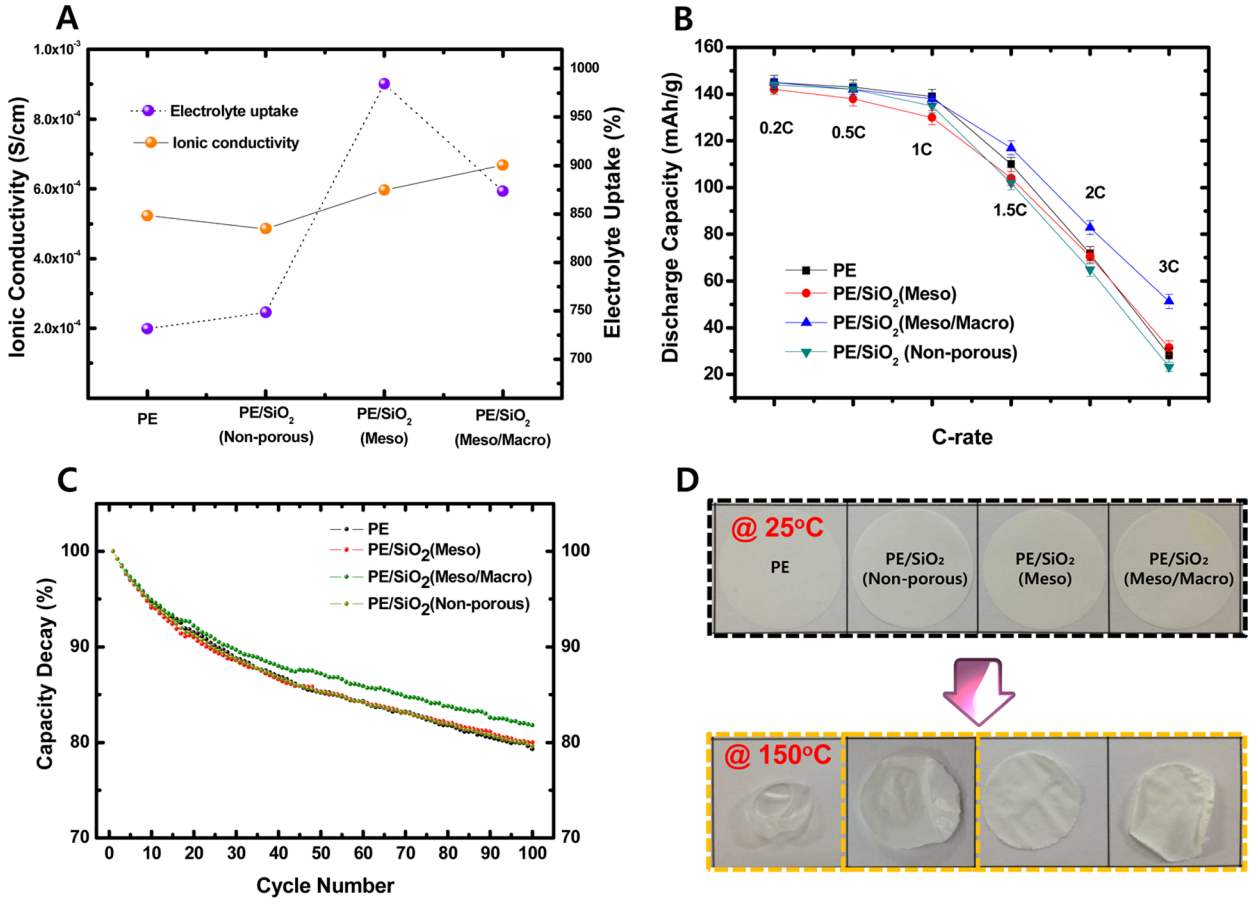

Figure 4. (A) Ionic conductivities and electrolyte uptakes of PE, meso-macroporous silica/PE, mesoporous silica particles/PE, and nonporous silica/PE separators. C-rate performances (B) and cyclabilities (C) of coin cells with PE, meso-macroporous silica/PE, mesoporous silica/PE, and nonporous silica/PE separators. (D) Thermal shrinkage results of PE, meso-macroporous silica/PE, mesoporous silica/PE, and nonporous silica/PE separators.

the conventional, nonporous nanoparticle system. If a PE substrate was coated by the porous silica nanoparticles, the coating layer would have an additional ionic path that could originate from the ionic path by the porous nanoparticle itself, as depicted in Figure 1B.

To understand how silica nanoparticles with multiscale pores can improve the thermal and mechanical properties of PE separators without detrimental effects, the surface morphologies of the silica nanoparticle-coated separators were compared with that of the pristine PE separator. In contrast to the neat PE separator (Figure S4), the composite separators [Figure 3(A, B) and (C, D)] had unique silica nanoparticle coating layers that were composed of closely packed highly porous silica nanoparticles interconnected by PVdF−HFP binders. As shown in Figure S4, the neat PE substrate had a very unique pore size of approximately several hundred nanometers. As expected from the different pore structures in the silica particles, two different types of pore structures were observed in the FE-SEM images (Figure 3). For instance, the mesoporous silica nanoparticles coating the PE separator (Figure 3A,B) were similar in arrangement to the nonporous silica nanoparticles (Figure S5). In contrast, the meso-macroporous silica exhibited a porous morphology in addition to well-connected interstitial voids between the silica nanoparticles. Although the mesoporous silica on the PE separator appears similar to nonporous silica in the SEM images, the high surface area of the mesoporous silica will be filled with liquid electrolytes and may provide an easy pathway for ion movement, thereby generating faster ion conductivity compared with nonporous silica structures. Presumably, the combination of macropores and mesopores in silica nanoparticles can boost Li ion transportation, thus minimizing the increase in ionic resistance that can result from the additional coating layer on the PE separator. The thickness of the silica nanoparticle coat was ~2.7 μm (Figure 3C, inset).

The electrolyte uptake behaviors of silica-coated PE separators with different particle morphologies are shown in Figure 4A. As predicted from the surface area data (Figure S2), the mesoporous silica-coated PE separator showed the highest liquid electrolyte uptake. Although the meso-macroporous silica/PE separator had relatively poor electrolyte uptake versus the mesoporous silica/PE separator, the ionic conductivity of the meso-macroporous silica/PE separator was the best, as shown in Figure 4A. Note that a coat of nonporous silica particles on a PE separator induces additional resistance, although these particles slightly enhance electrolyte uptake. Increasing the amounts of mesopores and macropores in silica nanoparticles can significantly affect the performance of LIBs, as shown by SEM observations and ionic conductivity analyses. The specific effect of the morphological differences between the composite separators on the electrochemical performance of LIBs was investigated. The discharge profiles of cells assembled with various silica-coated PE separators are shown in Figure S6. Coin cells were charged over a voltage range of 3.0−4.3 V at a

DOI: 10.1021/am506797d
ACS Appl. Mater. Interfaces 2015, 7, 4511−4517

constant current density of 0.2 C and discharged at different current densities ranging from 0.2 to 3 C. As the discharge current density increased, the voltage and discharge capacity of the coin cells tended to gradually decrease. This effect is caused by the increased serial resistance as the discharge C-rate increases. With respect to Li ion transportation, the pore structures of the inorganic nanoparticles coated on the PE separator and the wettability of the separator with a polar liquid electrolyte can both affect its ionic transportation. Since all coin cells were prepared from exactly the same electrodes, electrolyte, and fabrication conditions, any transportation differences must be due to variations in the separators that were used. The rate characteristics of the cells, including error bars, are shown in Figure 4B. Interestingly, the discharge capacities of the mesoporous silica/PE separator and the nonporous silica/PE separator were very similar to that of the neat PE separator. Most importantly, the separator coated with meso-macroporous SiO_2 showed a greater discharge capacity than all other silica-coated PE separators, as well as the PE separator itself (Figure 4B). The ionic transport resistance of a silica-coated PE separator is equal to the sum of the individual resistances; i.e. R(silica layer) + R(PE separator) + R(silica layer). By using meso-macroporous silica particles instead of nonporous silica particles or mesoporous particles, we minimized the resistance of the silica layer. This decreased resistance can explain why the meso-macroporous silica-coated PE separator exhibited enhanced C-rate performance compared with the other silica particle-coated PE separators. However, it cannot explain why the meso-macroporous silica-coated PE separator exhibited better performance than the PE separator. A previous study by Choi and co-workers speculated that improving the solvent wetting (affinities) using a polydopamine coating on the PE surface could significantly improve C-rate performances.[12] Our composite separators showed very high electrolyte uptake values compared with the PE separator. The main reason for this high uptake is presumably the high specific surface area of the silica nanoparticles. However, the high electrolyte uptake of the silica layer may also help the wetting behavior of the PE surface. Therefore, the interface between the silica layer and the PE surface, which is not present in a pure PE separator, may harbor significant amounts of electrolytes. The resulting improved electrolyte affinity can reduce the value of R(PE separator). Presumably, this positive effect is also observed in other silica-coated PE separators (nonporous silica/PE or mesoporous silica/PE). However, to achieve better C-rate performance than a PE separator, this positive effect must be combined with minimized silica resistance (R(silica layer)), such as that of meso-macroporous silica. Therefore, a well-designed multiscale porous structure in a composite separator can enable easy ionic conduction at high C-rate conditions.

The cyclabilities of the composite separators with silica-coated PE (meso-macroporous, mesoporous, and nonporous) and the PE separator are compared in Figure 4C. Cyclability was expressed as the discharge capacity as a function of cycle number. Coin cells were cycled between 3 and 4.2 V at a constant charge/discharge current density (1C/1C). The composite PE separator with nonporous silica exhibited much poorer discharge capacity retention after 100 cycles than the PE separator. Interestingly, the meso-macroporous silica-coated PE composite separator showed excellent discharge capacity retention after 100 cycles (Figure 4C); this retention was greater than that of the pristine PE separator and of the mesoporous silica-coated PE separator. Recently, PE separators coated with a ceramic layer (e.g., Al_2O_3 or SiO_2 powder) have been reported to retain liquid electrolytes better than a hydrophobic PE separator alone, thus improving cyclability.[17,18] As shown in Figure 4C, the coating of silica nanoparticles with a multiscale pore structure on a composite PE separator could be a promising alternative to commercialized PE separators in terms of long-term cycling. In inorganic nanoparticle-coated PE composite separators, the coated particle layer may add additional resistance for Li ion diffusion, although the layer can enhance liquid electrolyte uptake. For the mesoporous silica-coated PE separator, the advantage from the enhanced electrolyte uptake may be diminished by the additional resistance. As observed in the SEM images of the meso-macroporous silica-coated PE separator and the TEM images of the original silica nanoparticles, the small mesopores were well-connected with the large macropores. This structure generates a uniform ionic path throughout the separator while maintaining the electrolyte uptake of the separator. These unique features may be the primary reason for the improved cycle performance of the meso-macroporous silica-coated PE separator.

In general, the most important drawback of PE-based separators is their poor dimensional stability. Conventional PE separators have a melting point of approximately 135 °C and are prepared through multiple stretching processes that may cause internal short-circuiting when the temperature reaches or exceeds the melting point. The dimensional stability of the composite separators was observed by measuring their (area-based) dimensional changes after being subjected to high temperature (~150 °C) for 0.5 h (Figure 4D). As shown in Figure 4D, enhanced dimensional stability was observed for all silica-coated PE composite separators compared with that of the pristine PE separator. However, the thermal stability of the PE composite separators was dependent on the morphology of the inorganic nanoparticles coating the PE separator. The thermal shrinkages of the separators with nonporous and mesoporous silica nanoparticles were slightly less than that of the meso-macroporous silica-coated PE separator. Presumably, relatively small contact areas are present between the PE and inorganic particle surfaces and also between the inorganic nanoparticles themselves in the meso-macroporous silica/PE separators. The small contact area between the inorganic nanoparticles, resulting from the open pores in the surface of the meso-macroporous silica nanoparticles, could decrease the sustainable force that prevents the thermal shrinkage of the PE separator.

CONCLUSION

Here, we described how a simple solution dip-coating method can be used to coat a PE separator with silica nanoparticles exhibiting a multiscale pore structure. The resultant composite PE separators exhibited improved charge/discharge performance, cycle performance, and dimensional stability. To determine the effects of the inorganic nanoparticle coat on PE performance, inorganic silica nanoparticles with varying pore structures were generated, coated onto PE separators, and their performances compared with that of a conventional PE separator. Hierarchical pore structures enabled enhanced thermal stability, without sacrificing the electrochemical performance of the separator. This study introduces a new paradigm for Li-ion battery separators that can potentially be applied to EVs and HEVs.

DOI: 10.1021/am506797d
ACS Appl. Mater. Interfaces 2015, 7, 4511−4517

■ ASSOCIATED CONTENT

Supporting Information

Particle size distributions, BET adsorption−desorption curves, pore distributions, additional SEM images, and discharge profiles of coin cells. This material is available free of charge via the Internet at http://pubs.acs.org.

■ AUTHOR INFORMATION

Corresponding Authors

*E-mail: lutts@yonsei.ac.kr (J.H.P.).
*E-mail: yigira@skku.edu (G.-R.Y.).

Author Contributions

#These authors contributed equally to this work.

Notes

The authors declare no competing financial interest.

■ ACKNOWLEDGMENTS

This work was supported by the NRF of Korea Grant funded by the Ministry of Science, ICT and Future Planning (NRF-2013R1A2A1A09014038, 2009-0083540, NRF-2009-C1AAA001-2009-0094157, 2010-0029409). This work was also partially supported from the Ministry of Knowledge Economy (MKE) (20123010010070).

■ REFERENCES

(1) Xu, G.; Ding, B.; Nie, P.; Shen, L.; Dou, H.; Zhang, X. Hierarchically Porous Carbon Encapsulating Sulfur as a Superior Cathode Material for High Performance Lithium−Sulfur Batteries. *ACS Appl. Mater. Interfaces* **2014**, *6*, 194−199.

(2) Xu, G.; Ding, B.; Pan, J.; Nie, P.; Shen, L.; Dou, H.; Zhang, X. High Performance Lithium−Sulfur Batteries: Advances and Challenges. *J. Mater. Chem. A* **2014**, *2*, 12662−12676.

(3) Chen, J.; Cheng, F. Y. Combination of Lightweight Elements and Nanostructured Materials for Batteries. *Acc. Chem. Res.* **2009**, *42*, 713−723.

(4) Hu, Y.-S.; Demir-Cakan, R.; Titirici, M.-M.; Müller, J.-O.; Schlögl, R.; Antonietti, M.; Maier, J. Superior Storage Performance of a Si@SiOx/C Nanocomposite as Anode Material for Lithium-Ion Batteries. *Angew. Chem., Int. Ed.* **2008**, *47*, 1645−1649.

(5) Goodenough, J. B.; Kim, Y. Challenges for Rechargeable Li Batteries. *Chem. Mater.* **2010**, *22*, 587−603.

(6) Etacheri, V.; Marom, R.; Elazari, R.; Salitra, G.; Aurbach, D. Challenges in the Development of Advanced Li-ion Batteries: A Review. *Energy Environ. Sci.* **2011**, *4*, 3243−3262.

(7) Van Noorden, R. The Rechargeable Revolution: A Better Battery. *Nature* **2014**, *507*, 26−28.

(8) Hassoun, J.; Panero, S.; Reale, P.; Scrosati, B. A. A New, Safe, High-Rate and High-Energy Polymer Lithium-Ion Battery. *Adv. Mater.* **2009**, *21*, 4807−4810.

(9) Kim, M.; Park, J. H. Multi-Scale Pore Generation from Controlled Phase Inversion: Application to Separators for Li-Ion Batteries. *Adv. Energy Mater.* **2013**, *3*, 1417−1420.

(10) Arora, P.; Zhang, Z. J. Battery Separators. *Chem. Rev.* **2004**, *104*, 4419−4462.

(11) Ko, J. M.; Min, B. G.; Kim, D. W.; Ryu, K. S.; Kim, K. M.; Lee, Y. G.; Chang, S. H. Thin-Film Type Li-ion Battery, Using a Polyethylene Separator Grafted with Glycidyl Methacrylate. *Electrochim. Acta* **2004**, *50*, 367−370.

(12) Ryou, M. H.; Lee, Y. M.; Park, J. K.; Choi, J. W. Mussel-Inspired Polydopamine-Treated Polyethylene Separators for High-Power Li-Ion Batteries. *Adv. Mater.* **2011**, *23*, 3066−3070.

(13) Ryou, M. H.; Lee, D. J.; Lee, J. N.; Lee, Y. M.; Park, J. K.; Choi, J. W. Excellent Cycle Life of Lithium-Metal Anodes in Lithium-Ion Batteries with Mussel-Inspired Polydopamine-Coated Separators. *Adv. Energy Mater.* **2012**, *2*, 645−650.

(14) Bruce, P. G.; Scrosati, B.; Tarascon, J. M. Nanomaterials for Rechargeable Lithium Batteries. *Angew. Chem., Int. Ed.* **2008**, *47*, 2930−2946.

(15) Zhang, J.; Yue, L.; Kong, Q.; Liu, Z.; Zhou, X.; Zhang, C.; Xu, Q.; Zhang, B.; Ding, G.; Qin, B.; Duan, Y.; Wang, Q.; Yao, J.; Cui, G.; Chen, L. Sustainable, Heat-Resistant and Flame-Retardant Cellulose-Based Composite Separator for High-Performance Lithium Ion Battery. *Sci. Rep.* **2014**, *4*, 3935−3947.

(16) Jeong, H. S.; Lee, S. Y. Closely Packed SiO_2 Nanoparticles/Poly(vinylidene fluoride-hexafluoropropylene) Layers-Coated Polyethylene Separators for Lithium-Ion Batteries. *J. Power Sources* **2011**, *196*, 6716−6722.

(17) Wang, H.; Wu, J.; Cai, C.; Guo, J.; Fan, H.; Zhu, C.; Dong, H.; Zhao, N.; Xu, J. *ACS Appl. Mater. Interfaces* **2014**, *6*, 5602−5608.

(18) Jeong, H. S.; Hong, S. C.; Lee, S. Y. Effect of Microporous Structure on Thermal Shrinkage and Electrochemical Performance of Al_2O_3/Poly(vinylidene fluoride-hexafluoropropylene) Composite Separators for Lithium-Ion Batteries. *J. Membr. Sci.* **2010**, *364*, 177−182.

(19) Kang, S. M.; Ryou, M. H.; Choi, J. W.; Lee, H. Mussel- and Diatom-Inspired Silica Coating on Separators Yields Improved Power and Safety in Li-Ion Batteries. *Chem. Mater.* **2012**, *24*, 3481−3485.

(20) Kim, M.; Kim, Y. S.; Lee, Y. G.; Park, J. H. Solution Processable Silica Thin Film Coating on Microporous Substrate with High Tortuosity: Application to a Battery Separator. *RSC Adv.* **2013**, *3*, 16708−16713.

(21) Kim, M.; Park, J. H. Inorganic Thin Layer Coated Porous Separator with High Thermal Stability for Safety Reinforced Li-ion Battery. *J. Power Sources* **2012**, *212*, 22−27.

(22) Cho, Y. S.; Kim, Y. K.; Kim, S. H.; Lim, D. C.; Lee, J. G.; Baek, Y. K.; Yi, G. R. Spherical Meso-macroporous Silica Particles by Emulsion-Assisted Dual-Templating. *Mater. Exp.* **2014**, *4*, 91−104.

(23) Nandiyanto, A. B. D.; Suhendi, A.; Ogi, T.; Iwaki, T.; Okuyama, K. Synthesis of Additive-Free Cationic Polystyrene Particles with Controllable Size for Hollow Template Applications. *Colloids Surf., A* **2012**, *396*, 96−105.

(24) Brunauer, S.; Emmett, P. H.; Teller, E. Adsorption of Gases in Multimolecular Layers. *J. Am. Chem. Soc.* **1938**, *60*, 309−319.

(25) Barrett, E. P.; Joyner, L. G.; Halenda, P. P. The Determination of Pore Volume and Area Distributions in Porous Substances. I. Computations from Nitrogen Isotherms. *J. Am. Chem. Soc.* **1951**, *73*, 373−380.

DOI: 10.1021/am506797d
ACS Appl. Mater. Interfaces 2015, 7, 4511−4517